ISSN 1063-7761, Journal of Experimental and Theoretical Physics, 2008, Vol. 106, No. 1, pp. 172–181. © Pleiades Publishing, Inc., 2008.
Original Russian Text © I.A. Budagovsky, A.S. Zolot'ko, V.N. Ochkin, M.P. Smayev, A.Yu. Bobrovsky, V.P. Shibaev, M.I. Barnik, 2008, published in Zhurnal Éksperimental'noĭ i Teoreticheskoĭ Fiziki, 2008, Vol. 133, No. 1, pp. 204–214.

Orientational Optical Nonlinearity Induced by Comb-Shaped Polymers in a Nematic Liquid Crystal

I. A. Budagovsky[a], A. S. Zolot'ko[a], V. N. Ochkin[a], M. P. Smayev[a], A. Yu. Bobrovsky[b], V. P. Shibaev[b], and M. I. Barnik[c]

[a] *Lebedev Physical Institute, Russian Academy of Sciences, Moscow, 119991 Russia*
[b] *Moscow State University, Moscow, 119991 Russia*
[c] *Shubnikov Institute of Crystallography, Russian Academy of Sciences, Moscow, 117333 Russia*
e-mail: zolotko@lebedev.ru

Received July 3, 2007

Abstract—The effect of optical orientation in nematic liquid crystals containing small additions of high-molecular compounds, i.e., comb-shaped polymers with light-absorbing azobenzene side fragments, was studied. The effects of light-induced reorientation of the director of nematic liquid crystals caused by light absorption of polymers and a low-molecular compound with a structure similar to side fragments of the polymers were compared in detail. An explanation was proposed for large values of the orientational nonlinearity induced by polymers.

PACS numbers: 61.30.-v, 42.70.Df, 82.35.Ej, 42.65.Jx

DOI: 10.1134/S1063776108010159

1. INTRODUCTION

Liquid-crystal phases represent a form of "soft matter" [1]. Their high sensitivity to various external perturbations [2, 3] leads, in particular, to very strong optical orientation effects. For example, a light wave passing through a transparent nematic liquid crystal (NLC) causes director **n** reorientation [4–6]. In this case, the threshold power density for the Freedericksz transition is only ~10^3 W/cm^2 [6].

Director rotation changes the refractive index of an extraordinary wave, thus causing orientational nonlinearity of NLCs. The corresponding "giant" orientational optical nonlinearity exceeds the Kerr nonlinearity of ordinary liquids by nine orders of magnitude [5].

Reorientation of molecules of transparent NLCs is caused by the direct force action of a light field on dipoles induced by the same field; the torque per NLC unit volume is given by

$$\mathbf{\Gamma} = \frac{\zeta |A|^2}{8\pi}(\mathbf{n}\cdot\mathbf{e})[\mathbf{n}\times\mathbf{e}], \qquad (1)$$

where the parameter ζ is equal to the optical anisotropy $\Delta\varepsilon$, A is the light field amplitude, and **e** is the light polarization unit vector. Since $\Delta\varepsilon$ is positive, the director rotates to align parallel to the light field and hence, the refractive index for the extraordinary wave increases ("positive" nonlinearity).

A small addition (~1 wt %) of dye molecules can significantly increase the efficiency of the orientational effect of light (the nonlinearity can additionally increase by two orders of magnitude) [7, 8]. The torque acting on the director of an absorbing NLC is also described by relation (1), in which, however, the parameter ζ should be understood as a certain quantity $\Delta\varepsilon_{\text{eff}}$ referred to as the effective optical anisotropy. In this case, depending on the dye type and experimental configuration, $\Delta\varepsilon_{\text{eff}}$ can be both positive and negative; i.e., the director can rotate both parallel and perpendicularly to the light field [9, 10] (in the latter case, the refractive index decreases and the crystal exhibits negative orientational nonlinearity). The nonlinear-optical response of absorbing NLCs can be characterized by the ratio $\eta = \Delta\varepsilon_{\text{eff}}/\Delta\varepsilon$, called the nonlinearity enhancement factor.

Currently, physical mechanisms of orientation effects in absorbing NLCs are a subject of study. It is commonly accepted that the director rotation occurs due to changes in intermolecular force strength in an NLC sample when introduced dye molecules are excited [8].

Orientational nonlinearities allow the observation and study of various effects (e.g., the aberrational self-action of light beams [6, 11–14], wave phase conjugation [15–22], formation and interaction of optical solitons [23–29], appearance of periodic and stochastic

oscillations of the director field [30–38], optical bistabilities [39–45], and others) at very low power densities of light waves.

So far, almost exclusively low-molecular dyes have been used as additions inducing orientational nonlinearity associated with changes in intermolecular forces. It has remained unclear how complication of the molecular structure can affect optical orientation effects. Light-induced director reorientation caused by a high-molecular compound, i.e., the conjugated polymer MEH–PPV, was first observed in [46]. The corresponding orientational nonlinearity was negative independently of the experimental configuration, and its magnitude exceeded the nonlinearity of the initial (undoped) nematic matrix by an order of magnitude.

Large orientational optical nonlinearity induced by comb-shaped polymer P1 in the nematic matrix was observed in [47]; this nonlinearity exceeded that induced by low-molecular azo compound AD, whose structure is similar to side fragments of the polymer. In this paper, we present experimental results on the effect of light on liquid-crystal systems with added comb-shaped polymers P1 and P2 differing by lengths of links bonding azo fragments with the polymeric chain. The orientational nonlinearities induced by polymers and the low-molecular azo compound were compared in detail. An explanation was proposed for an increase in the nonlinearity as the molecular structure becomes more complex.

2. EXPERIMENTAL CONDITIONS AND SAMPLES

The structural formulas of comb-shaped polymers P1 (molecular mass $M = 4.7 \times 10^4$) and P2 ($M = 7 \times 10^3$) are written as

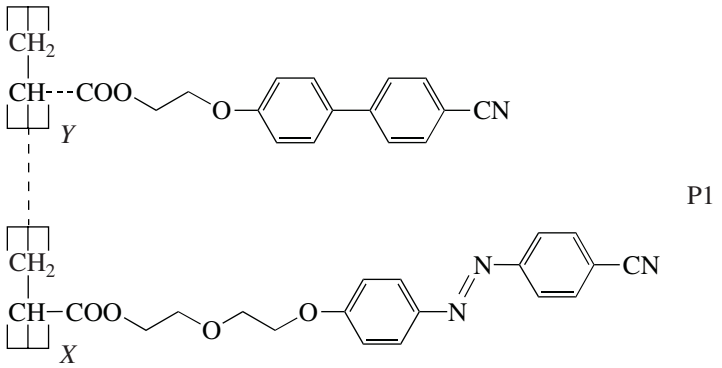

P1

(Fraction $X = 60\%$ and $Y = 40\%$),

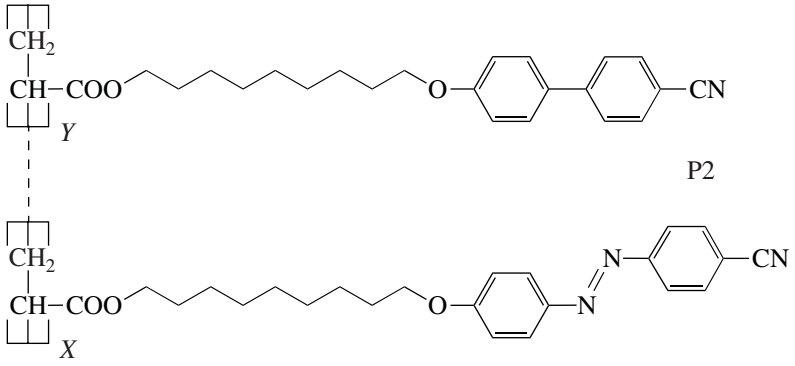

P2

(Fraction $X = 40\%$ and $Y = 60\%$).

The polymers contain cyanobiphenyl and azo fragments attached to the alkyl chain by oxyaliphatic (P1) and aliphatic (P2) links with different lengths. The choice of polymers containing azo groups as an object of study is explained by the fact that excitation of the double bond of azobenzene chromophore by light can cause strong orientation effects due to changes in intermolecular forces. Such effects are known, e.g., for mixtures of low-molecular azo compounds with viscous liquids [48, 49], nematic matrices [10, 12, 50], and various liquid-crystal phases of polymers [51, 52].

The structural formula of the used low-molecular azo dye AD similar to side azo fragments of polymers is written as

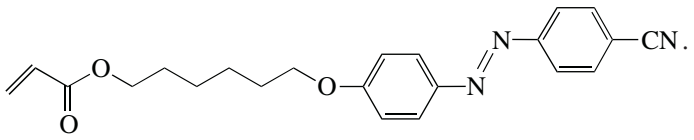

The absorption maxima of polymers and azo dye AD are in the ultraviolet region of the spectrum. In the blue–green region (λ = 440–550 nm), the absorbance of these compounds monotonically decreases with increasing light wavelength. For example, for a 0.5% solution of P1 in the ZhKM-1277 nematic matrix, the absorbances are $\alpha_{\parallel}$ = 51, 43, 33, 14 cm^{-1} and $\alpha_{\perp}$ = 13, 11, 8, 3 cm^{-1} for wavelengths λ = 458, 473, 488, and 515 nm, respectively. The same absorbances were obtained for sample ZhKM-1277 + 0.3% AD with almost the same concentration of azo fragments. For a 0.5% solution of P2 in the ZhKM-1277 matrix, $\alpha_{\parallel}$ = 23 cm^{-1} and $\alpha_{\perp}$ = 8 cm^{-1} (λ = 473 nm).

The ZhKM-1277 nematic matrix (developed by the Research Institute of Organic Intermediates and Dyes, Russia) used in the experiments is a mixture of biphenyls and esters. It forms a nematic phase in a wide temperature range (–20°C to 60°C) and is characterized by positive low-frequency dielectric anisotropy. The refractive indices of extraordinary and ordinary waves for ZhKM-1277 are $n_{\parallel}$ = 1.71 and $n_{\perp}$ = 1.52 (λ = 589 nm), respectively. We note that the presence of side cyanobiphenyl groups in polymers P1 and P2 provided their good solubility in this matrix.

The study was performed with liquid-crystal mixtures containing 0.1, 0.5, and 2% of P1; 0.5% of P2; and 0.3% of azo compound AD. Planar and homeotropically oriented cells of thickness L = 100 μm were used.

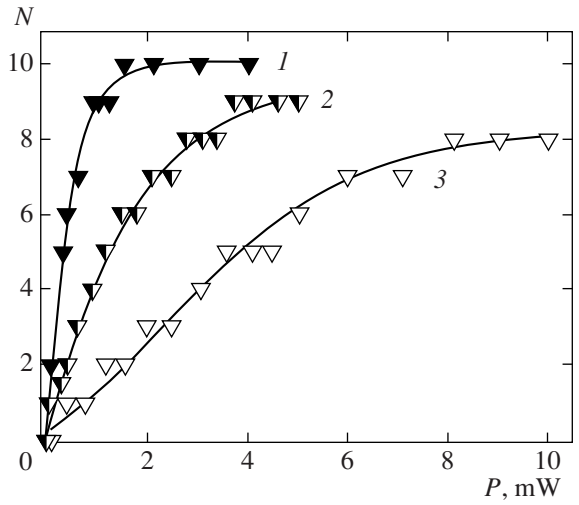

Fig. 1. Dependences of the number of aberration rings N of self-defocusing on the power P of the light beam (λ = 473 nm, α = 50°) transmitted through homeotropically oriented samples ZhKM-1277 with (*1*) 0.5% of polymer P1, (*2*) 0.5% of polymer P2, and (*3*) 0.3% of dye AD added.

Inner cell walls were coated with conducting layers of indium oxide and tin oxide, which allowed us to apply a low-frequency electric field to samples, thus varying the angle δ between **n** and **E** [53].

Argon and solid-state lasers emitting at wavelengths λ = 458, 473, 476, 488, 515, and 532 nm were used as radiation sources. The light beam was focused into the NLC by a lens with focal length f = 18 cm. The beam polarization plane was rotated using a Fresnel double rhomb. The liquid-crystal layer plane was vertical; the unperturbed director $\mathbf{n}_0$ lay in the horizontal plane. The angle α of light incidence on the crystal could be varied by rotating the cell with the NLC about the vertical axis. The light beam transmitted through the NLC was observed on a screen.

The light-induced change in the refractive index was studied using the light beam self-action appearing in the formation of a characteristic system of aberration rings in the beam cross section [6, 11]. The number of aberration rings N is related to the sample-thickness-average change Δn in the refractive index of the extraordinary wave by the simple relation $\Delta n = N\lambda/L$. The sign of the light-induced refractive index (i.e., in fact, the director rotation direction) was determined by the aberration pattern transformation when the NLC was shifted perpendicularly to the incident light beam axis [12].

3. RESULTS

A characteristic aberration pattern arose when ZhKM-1277 crystals doped with polymers or azo dye were irradiated. The pattern nature was orientational, which was suggested by the dynamics of its formation and relaxation; the formation time was τ_d ~ 20 s–1 min (depending on the radiation power and the angle of light incidence); the relaxation time was τ_r ~ 15 s.

The determination of the self-action sign showed that light beam self-defocusing (negative nonlinearity) occurs in polymer-doped samples (homeotropic and planar) and a homeotropically oriented sample containing AD. A corresponding decrease in the refractive index of the extraordinary wave is obviously caused by director **n** rotation perpendicular to the light field **E**. In the case of the planar oriented AD-doped crystal, light beam self-focusing was observed (positive nonlinearity; the refractive index increases due to the director **n** rotation parallel to the field **E**).

Observation of self-defocusing unambiguously shows the relation of orientation effects in the liquid-crystal systems under study with the presence of absorbing additions.

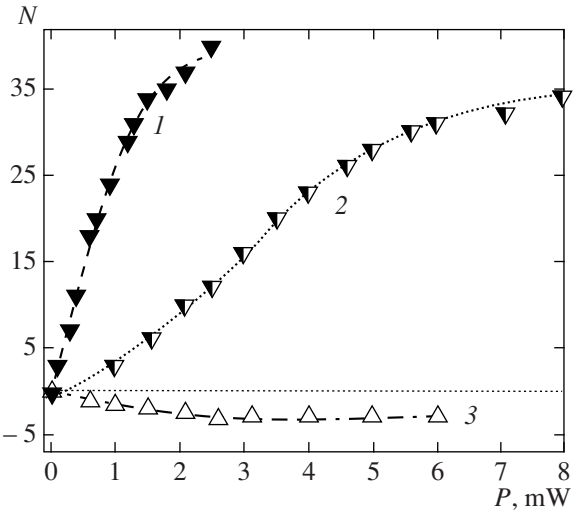

Fig. 2. Dependences of the number of aberration rings N on the power P of the light beam ($\lambda = 473$ nm, $\alpha = 50°$) transmitted through the planar oriented samples ZhKM-1277 with an added (*1*) 0.5% of polymer P1 (beam self-defocusing), (*2*) 0.5% of polymer P2 (beam self-defocusing), and (*3*) 0.3% of dye AD (self-focusing).

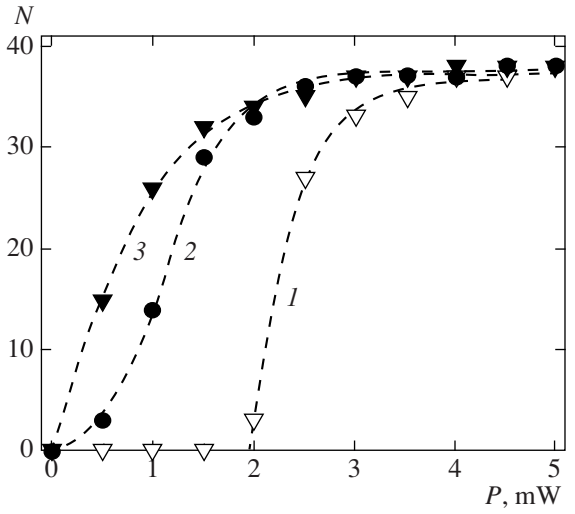

Fig. 3. Dependences of the number of aberration rings N of self-defocusing on the power P of the light beam ($\lambda = 476$ nm) transmitted through the planar oriented sample ZhKM-1277 + 0.5% P1 at incidence angles $\alpha = 0$, 20°, and 40° (curves *1–3*, respectively).

The dependences of the number of aberration rings N on the light beam power P are shown in Figs. 1 and 2. We can see that an increase in P leads to a monotonic increase and saturation of N. It is also seen in Fig. 1 that, outside the saturation region, the negative nonlinear-optical response caused by the presence of polymer P1 is approximately five times larger than the response induced by P2 and approximately ten times larger than that for "free" azo dye molecules. Most experiments were carried out with polymer P1 (systematic features for the crystal containing P2 are similar; only nonlinear-optical responses differ).

Figure 3 shows the dependences of the number of aberration rings N on the light beam power P for various angles α of light incidence on the P1-doped planar NLC. We can see that director reorientation at normal light incidence ($\alpha = 0$) has a threshold of $P_{th} = 1.9$ mW. A similar behavior was observed for the P2-doped planar sample; the threshold power was $P_{th} = 17.5$ mW. It should be noted that the orientational self-action of the light beam did not develop at normal light incidence on homeotropic samples and on the AD-doped planar crystal since the director **n** in these experimental configurations is initially oriented in the same direction in which the light field **E** attempts to rotate it.

At a sufficiently large power P, the number of aberration rings N approaches the maximum value N_{sat} in the saturation region (Figs. 1–3), which corresponds to a full rotation of the director **n** to align it perpendicularly or parallel to the light field. For example, at normal incidence of the light beam on the planar NLC (Fig. 3, curve *1*), $N_{sat} = 37$. The maximum possible number of rings, estimated for $\Delta n = 0.19$ on full rotation of the director **n** about the beam axis to align perpendicularly to **E**, is $N_{max} = 40$.

We note that systematic features of light-induced director reorientation in NLCs with added polymers (the threshold at normal incidence and reorientation saturation) are the same as in the case of the light-induced Freedericksz transition in transparent (undoped) homeotropic NLCs [6, 54].

The efficiency of the effect of the light field increases as the polymer P1 concentration increases or as the light wavelength decreases. For example, as c_p increases from 0.1 to 2%, the threshold power P_{th} of director reorientation decreases from 7 to 0.6 mW (planar crystal, $\lambda = 473$ nm). The P_{th} decrease slower than the concentration c_p increase can be explained by an increase in the light wave damping. At $c_p = 0.5\%$, a decrease in the wavelength from 515 to 476 nm results in an approximately threefold decrease in P_{th}, which is apparently caused by changes in light absorbances.

The nonlinear-optical response induced by polymer P1 and azo dye AD in the extraordinary light wave field was quantitatively determined. To this end, light beam powers at which identical nonlinear-optical responses of the liquid-crystal system were observed were compared in the same configurations of the interaction between the NLC director and light field (the threshold powers of the Freedericksz transition or the powers at which identical numbers of aberration rings are observed were used as compared values). In the case of a negative (induced by additions) nonlinearity, the responses in NLCs with different orientations (for example, the Freedericksz transition threshold in

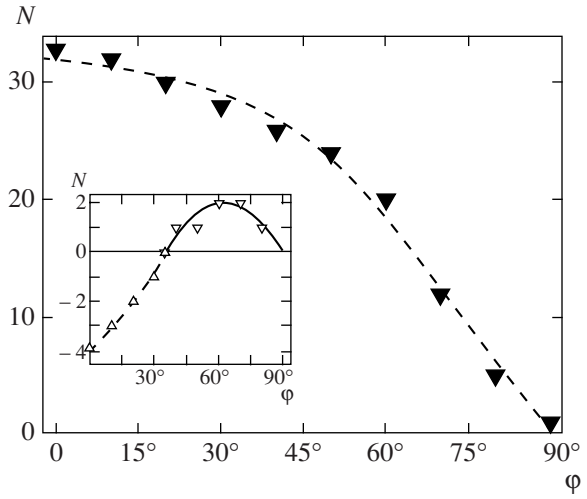

Fig. 4. Dependence of the number of aberration rings N of self-defocusing on the angle φ of rotation of the plane of polarization for the planar sample ZhKM-1277 + 0.5% P1 (λ = 473 nm, P = 4 mW, α = 60°). The inset shows the dependence N(φ) for planar ZhKM-1277 + 0.3% AD (λ = 473 nm, P = 4 mW, α = 60°); inverted and upright triangles correspond to beam self-defocusing and self-focusing, respectively.

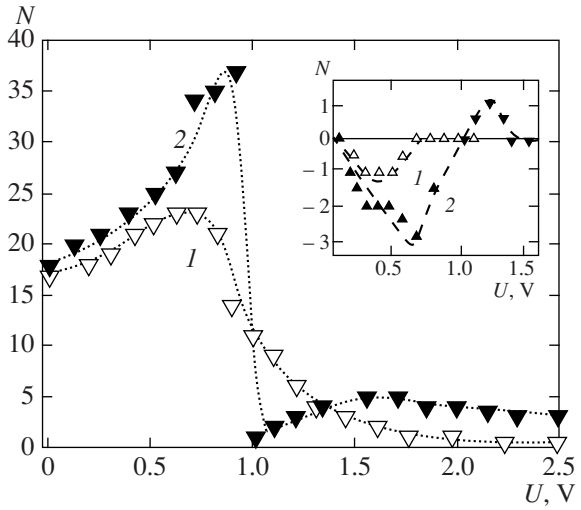

Fig. 5. Dependences of the number of aberration rings N of self-defocusing on the low-frequency (ν = 3 kHz) voltage U for the planar oriented sample ZhKM-1277 + 0.5% P1 (λ = 473 nm, P = 1 mW) at incidence angles α = 40° and –40° (curves *1* and *2*, respectively). The inset shows the dependence N(U) for planar ZhKM-1277 + 0.3% AD (λ = 473 nm, P = 1 mW) at α = 40° and –40° (curves *1* and *2*, respectively); inverted triangles correspond to beam self-defocusing and upright triangles correspond to beam self-focusing.

undoped homeotropic and doped planar NLCs) were compared.

For λ = 488 nm, the threshold of the light-induced Freedericksz transition in the planar sample ZhKM-1277 + 0.5% P1 is P_{th} = 2 mW. The transition threshold in the homeotropically oriented sample of the undoped ZhKM-1277 matrix with the same thickness is P_{th} = 115 mW. The corresponding nonlinearity enhancement factor (defined in the Introduction) is η = –57.5. A comparison of the dependences N(P) measured at α = 50° and λ = 473 nm for homeotropic and planar samples of ZhKM-1277 + 0.1% P1 with the corresponding dependences for pure NLCs yielded the value η = –30. In the case of AD-doped NLCs, at α = 50° and λ = 473 nm, the values η = 10 and –12.5 were obtained for planar and homeotropic samples, respectively. For planar and homeotropic samples doped with 0.5% P2, η = –20 and –10, respectively (α = 50° and λ = 473 nm).

Figure 4 shows the dependence of the number of rings N on the angle φ of rotation of the plane of polarization (with respect to the horizontal plane) for the light beam transmitted through the NLC. In case of planar sample ZhKM-1277 + 0.5% P1, we can see that the transition from horizontal polarization (φ = 0, *e* wave) to vertical polarization (φ = 90°, *o* wave) results in the aberration pattern "collapse" (N decreases from 33 to 0). A similar dependence is observed during irradiation of the sample containing P2. However, the dependence of the light self-action on its polarization for planar sample ZhKM-1277 + 0.3% AD (inset in Fig. 4) differs essentially. In this case, the rotation of the plane of polarization leads to a change in the self-action sign (self-focusing is changed to self-defocusing).

A fundamental difference also exists when a low-frequency (ν = 3 kHz) field is applied to planar NLCs with added comb-shaped polymers and AD. In the case of ZhKM-1277 + 0.5% P1 (Fig. 5) and ZhKM-1277 + 0.5% P2, light beam self-defocusing is continuously observed as the voltage U increases. The dependence of N(U) is nonmonotonic; its shape depends on the sign of the angle α (curves *1* and *2*). Application of an external low-frequency voltage to the planar crystal doped with AD molecules (inset in Fig. 5) results in a self-action sign change at negative α (curve *2*). At positive α, the self-action (self-focusing) sign is unchanged.

Application of a low-frequency field to homeotropic NLCs leads to a monotonic decrease in N (suppression of the director field deformation) independently of sample composition.

4. DISCUSSION

Thus, negative nonlinearity is observed in NLCs with added comb-shaped polymers P1 and P2 independently of the experimental geometry (angle δ between **E** and **n**). Indeed, self-defocusing was also observed in homeotropic and planar samples for an extraordinarily polarized wave, including the case of the presence of a low-frequency electric field. Application of a low-frequency electric field to the planar NLC allowed the determination of the nonlinearity sign at angle δ values

unattainable in planar and homeotropic samples due to light refraction at their boundaries ($32° \le \delta \le 58°$). In this case, the difference between the dependences $N(U)$ for positive and negative angles α (Fig. 5) is caused by the director pretilt, which sets a well-defined rotation direction **n** under a low-frequency field [53]; at sufficiently large U, the director in the NLC volume is oriented perpendicularly to walls and light-induced reorientation is suppressed. In the case of the interaction of light with the superposition of extraordinary and ordinary waves (Fig. 4), the nonlinearity was also negative.

Let us compare the nonlinearity induced by polymer P1 with the results previously obtained for other liquid-crystal systems. First, we note that the nonlinearity enhancement factor η is proportional to the absorbing molecule concentration; therefore, it is reasonable to characterize the nonlinear-optical response by the ratio of the factor η to the absorbance $\eta' = \eta/\alpha$ or, e.g., by the quantity $\eta_\alpha = \eta/(\alpha_\parallel + 2\alpha_\perp)$, proportional to the ratio of the factor η to the absorbance $\alpha_{av} = (\alpha_\parallel + 2\alpha_\perp)/3$ averaged over director orientations. The advantage of the quantity η_α is its independence from the experimental configuration in the case of a constant conformational composition of chromophores.

For the liquid-crystal system with polymer P1, the parameter $\eta = -30$ measured at $\lambda = 473$ nm in the case of oblique incidence corresponds to $\eta_\alpha = -2.3$ cm (the values of η' for homeotropic and planar NLCs are –8 and –3.9 cm). The parameter η_α determined at $\lambda = 488$ nm by the Freedericksz transition threshold is smaller by a factor of 2.5. In the case of planar and homeotropic samples ZhKM-1277 + 0.5% P2, $\eta_\alpha = -0.5$ and –0.25 cm, respectively ($\lambda = 473$ nm).

The nonlinearity parameter $\eta_\alpha = -2.3$ cm in magnitude exceeds the maximum (to our knowledge) value $\eta_\alpha = -0.05$ cm for negative nonlinearity by more than ten times (calculated by the data of [9], where nonlinearity was induced by anthraquinone dye D4). It also exceeds the maximum value for positive nonlinearity, $\eta_\alpha = 0.8$ cm (calculated by the parameter $\eta' = 3.4$ cm [55]; the nonlinearity was caused by oligothiophene TR5).

Let us now consider the nonlinearity induced by low-molecular dye AD. As noted above, AD belongs to the class of azo compounds. Previously, a sign-alternating nonlinearity dependent on the angle δ was observed in NLCs with dyes of this class [10, 12, 50, 56]. This effect is due to different properties of trans and cis isomers of azo molecules. The presence of trans and cis isomers in the nematic matrix induces negative and positive nonlinearity, respectively. Without irradiation, molecules are mostly in the trans state. Absorption of light photons increases the concentration of cis isomers, and the ratio of isomer concentrations becomes dependent on δ (this dependence is caused by the smaller orientational order parameter of cis isomers in the nematic matrix). As a result, as δ increases, the nonlinearity changes sign from plus to minus at a certain critical value δ_c.

Precisely this effect explains the results obtained for NLCs with added AD. The sign change from plus to minus occurred as δ increased during the transition from planar to homeotropic orientation under a low-frequency field applied to the planar NLC (inset in Fig. 5) and during rotation of the plane of polarization, i.e., the transition from extraordinary wave to ordinary wave (inset in Fig. 4).

The critical angle δ_c can be estimated using the relation

$$\varphi_c = \arccos\left(\frac{\sin\delta_c}{\sin\delta}\right), \qquad (2)$$

where φ_c is the critical angle of rotation of the plane of polarization, at which the sign of the dependence $N(\varphi)$ changes. It is $\varphi_c = 35°$ (inset in Fig. 4), and the refraction angle δ determined from Snell's law (for the angle of incidence $\alpha = 60°$) is 58°. This results in $\delta_c = 44°$.

We now turn to the possible causes of the difference between nonlinearities induced by polymers and "free" azo molecules. Exact determination of these causes requires detailed information on the photoconformational activity and rotational diffusion of polymer fragments and azo molecules, their spatial arrangement with respect to nematic matrix molecules, changes in intermolecular potentials during absorption of light photons, and so on. Nevertheless, some assumptions can be stated on the basis of the models of nonlinearity sign alternation [50] and light-induced director reorientation [57].

According to [50], the nonlinearity induced by azo compounds depends on the ratio of concentrations of trans and cis isomers, in turn dependent on their photoisomerization cross sections and the orientational order parameters.

However, the processes of photoisomerization of azo compounds should be mainly controlled by a molecule part directly bound with the azo group, and it is identical for azo fragments of polymers and AD molecules. Therefore, the problem of the effect of molecular structure complication on the ratio of isomers in a light field requires independent study. In the case at hand, the effect of links on the order parameters seems improbable due to the above-mentioned identity of absorption spectra of polymer P1 and AD molecules.

In our opinion, an important role in the nonlinearity enhancement is played by the difference in the symmetry of the arrangement of nematic matrix molecules with respect to the "free" molecule and bound fragment; the "free" molecule is surrounded by matrix mol-

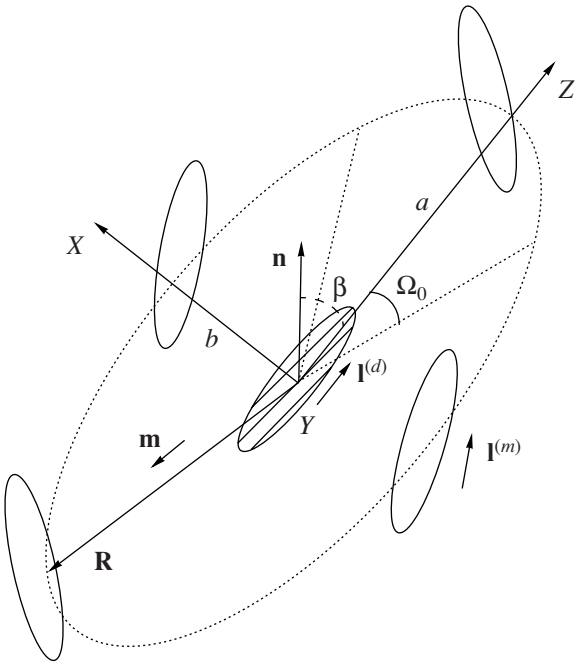

Fig. 6. Geometry of the interaction of excited dye molecules or polymer fragment with surrounding molecules of the nematic matrix: $\mathbf{l}^{(d)}$ and $\mathbf{l}^{(m)}$ are unit vectors parallel to the major axes of dye molecules (the fragment) and the matrix; **R** is the radius vector connecting the centers of dye molecules (the fragment) and the matrix, $\mathbf{m} = \mathbf{R}/R$; **n** is the NLC director; β is the angle between the major axis of the dye molecule and the director; a and b are the semimajor and semiminor axes of the ellipsoid of revolution, on which matrix molecules can be arranged; Ω_0 is the polar angle within which (in the case of polymer) matrix molecules cannot be arranged.

ecules on all sides; in the case of side azobenzene groups of polymers, this is hampered by the polymer backbone.

Let us explain this in more detail. According to [57], the light-induced director reorientation is caused by the torque occurring due to changes in intermolecular forces during orientation-selective excitation of molecules by polarized light. In this case, the necessary condition for such a torque is the eccentricity of the intermolecular interaction potential [58].

Let us first consider the moment arising during excitation of a "free" dye molecule. Let the direction of its major axis be set by the unit vector $\mathbf{l}^{(d)}$ (Fig. 6). The dispersion interaction potential between fluctuation dipole moments of dye molecules and the nematic matrix is given by

$$U^{(d,m)} = -\frac{B}{R^6}[(\mathbf{l}^{(d)}\cdot\mathbf{l}^{(m)})^2 - 6(\mathbf{l}^{(d)}\cdot\mathbf{l}^{(m)}) \times(\mathbf{m}\cdot\mathbf{l}^{(d)})(\mathbf{m}\cdot\mathbf{l}^{(m)}) + 9(\mathbf{m}\cdot\mathbf{l}^{(d)})^2(\mathbf{m}\cdot\mathbf{l}^{(m)})^2], \quad (3)$$

where B is the coefficient depending on the quantum molecular state of the dye, $\mathbf{l}^{(m)}$ is the unit vector parallel to the major axis of the matrix molecule, and $\mathbf{m} = \mathbf{R}/R$, where $\mathbf{R} = \mathbf{r}_m - \mathbf{r}_d$ is the vector connecting the dye and matrix molecule centers.

The eccentricity of potential (3), i.e., the nonparallelism of forces acting on dye molecules ($\mathbf{F}^{(d)} = -\partial U^{(d,m)}/\partial \mathbf{r}_d$), matrix molecules ($\mathbf{F}^{(m)} = -\partial U^{(d,m)}/\partial \mathbf{r}_m$), and the vector **R**, leads to the formation of a nonzero torque acting on the pair of molecules under consideration,

$$\mathbf{M}^{(d,m)} = \left[\mathbf{m}\times\frac{\partial U^{(d,m)}}{\partial \mathbf{m}}\right]. \quad (4)$$

The change in this moment caused by dye molecule excitation (the change ΔB in the coefficient B in (3)) is given by

$$\Delta\mathbf{M}^{(d,m)} = \frac{6\Delta B}{R^6}((\mathbf{l}^{(d)}\cdot\mathbf{l}^{(m)}) - 3(\mathbf{m}\cdot\mathbf{l}^{(d)}) \times(\mathbf{m}\cdot\mathbf{l}^{(m)}))((\mathbf{m}\cdot\mathbf{l}^{(m)})[\mathbf{m}\times\mathbf{l}^{(d)}] + (\mathbf{m}\cdot\mathbf{l}^{(d)})[\mathbf{m}\times\mathbf{l}^{(m)}]). \quad (5)$$

The value of $\Delta\mathbf{M}^{(d,m)}$ should be averaged over the relative orientation of dye and matrix molecules. To this end, let us assume that the centers of neighboring matrix molecules (we suppose that their number is equal to $N_n \sim 6$) are equiprobably arranged on the surface of the ellipsoid of revolution (prolate along $\mathbf{l}^{(d)}$, see Fig. 6) with semiaxes a and b ($a > b$). In this case, the averaged moment is written as

$$\langle\Delta\mathbf{M}^{(d,m)}\rangle = \frac{N_n}{S_{\rm el}}\int_S \Delta\mathbf{M}^{(d,m)}dS, \quad (6)$$

where integration is performed over the ellipsoid surface and $S_{\rm el}$ is the area of this surface. Let us introduce a coordinate system whose Z axis is parallel to the major axis of the dye molecule (vector $\mathbf{l}^{(d)}$); the X axis is perpendicular to the Z axis and lies in the plane defined by $\mathbf{l}^{(d)}$ and the director **n**, and the Y axis is perpendicular to the plane XZ (Fig. 6). In this coordinate system, assuming for simplicity that $\mathbf{l}^{(m)} = \mathbf{n}$,

$$\begin{aligned} &l_x^{(d)} = 0, && l_y^{(d)} = 0,\\ &l_z^{(d)} = 1, && l_x^{(m)} = \sin\beta,\\ &l_y^{(m)} = 0, && l_z^{(m)} = \cos\beta,\\ &m_x = \sin\Omega\cos\varphi, && m_y = \sin\Omega\sin\varphi,\\ &m_z = \cos\Omega, \end{aligned} \quad (7)$$

where β is the angle between $\mathbf{l}^{(d)}$ and **n**; Ω and φ are the polar and azimuthal angles.

Substituting (7) into (6), we obtain

$$\langle\Delta\mathbf{M}^{(d,m)}\rangle = \frac{3\Delta B}{b^6}g(\mu)(\mathbf{l}^{(m)}\cdot\mathbf{l}^{(d)})[\mathbf{l}^{(m)}\times\mathbf{l}^{(d)}], \quad (8)$$

where

$$g(\mu) = \left\{\int_0^\pi d\Omega \sin\Omega(1-\mu\cos^2\Omega)\right.$$

$$\left.\times(1-\mu(2-\mu)\cos^2\Omega)^{1/2}(15\cos^4\Omega - 12\cos^2\Omega + 1)\right\} \quad (9)$$

$$\times\left\{\int_0^\pi d\Omega \sin\Omega \frac{(1-\mu(2-\mu)\cos^2\Omega)^{1/2}}{(1-\mu\cos^2\Omega)^2}\right\}^{-1}$$

and $\mu = (a^2 - b^2)/a^2$. Expression (8) obviously holds true for an arbitrary orientation of the matrix molecule. The probability that the dye molecule is in the excited state (under the assumption that its absorption oscillator is parallel to $\mathbf{l}^{(d)}$) is given by

$$w(\mathbf{l}^{(d)}) = \frac{S_p\tau^*\sigma_0}{\hbar\omega}(\mathbf{e}\cdot\mathbf{l}^{(d)})^2, \quad (10)$$

where $S_p = cn|A|^2/8\pi$ is the Poynting vector, $\mathbf{e}$ is the polarization vector, ω is the frequency, n is the refractive index, A is the complex amplitude of the light wave, $\sigma_0 = (\alpha_\parallel + 2\alpha_\perp)/c_d$, c_d is the dye molecule concentration, and τ^* is the minimum of the two times (i.e., the dye molecule lifetime in the excited state and the rotational diffusion time). Additionally multiplying (8) by (10) and c_d and then averaging over the dye and matrix molecule orientation, we arrive at expression (1) with

$$\zeta = \Delta\varepsilon_{\text{eff}} = \frac{2N_n\Delta B g(\mu) cn\tau^*(\alpha_\parallel + 2\alpha_\perp)S_m(7 + 5S_d - 12S'_d)}{35b^6\hbar\omega}, \quad (11)$$

where $S_d = \langle P_2((\mathbf{n}\cdot\mathbf{l}^{(d)})^2)\rangle$, $S_m = \langle P_2((\mathbf{n}\cdot\mathbf{l}^{(m)})^2)\rangle$, and $S'_d = \langle P_4((\mathbf{n}\cdot\mathbf{l}^{(d)})^2)\rangle$ are the order parameters of dye and matrix molecules, expressed in terms of averaged Legendre polynomials.

It follows from (9) and (11), $\Delta\varepsilon_{\text{eff}} = 0$ at $a = b$. Thus, the necessary condition of the appearance of optical nonlinearity is correlation function anisotropy, i.e., the dependence of the distance between molecules with given orientations of major axes on the direction. Using (11) and the values $N_n = 6$, $\Delta B/a^6 \sim k_B T \sim 4\times10^{-14}$ erg, $c = 3\times10^{10}$ cm/s, $n = 1.5$, $\tau^* \sim 10^{-8}$ s, $\hbar\omega = 4\times10^{-12}$ erg ($\lambda = 473$ nm), $S_m \sim S_d \sim S'_d \sim 0.5$, and $g = 1$, we estimate the parameter $\eta_\alpha = \Delta\varepsilon_{\text{eff}}/\Delta\varepsilon(\alpha_\parallel + 2\alpha_\perp)$ as $\eta_\alpha \sim 3$, which corresponds to experimental data in order of magnitude.

Expression (11) relates to low-molecular dye molecules ("free" azo fragments). In the case of polymer, surrounding molecules of the nematic matrix are not distributed within the total solid angle 4π (this is prevented by the polymer chain). To estimate the effect of this factor, integration over the polar angle Ω in (9) should be performed in the range $\Omega_0 < \Omega < \pi$, rather than from 0 to π. In this case, the factor g in (11) becomes nonzero even at $\mu = 0$,

$$g = \frac{3\cos^5\Omega_0 - 4\cos^3\Omega_0 + \cos\Omega_0}{2}. \quad (12)$$

In the first nonvanishing in μ and Ω_0 approximation, $g = -\Omega_0^2 - 16\mu/105$. Hence, azo fragment attachment to the polymer chain can increase the orientational nonlinearity.

The difference between nonlinearities induced by polymers P1 and P2 is obviously caused by the difference between lengths of links connecting chromophores with the alkyl chain. Shorter links of P1 to a greater extent limit the arrangement of matrix molecules around chromophores, which causes greater nonlinearity.

We note that the explanation of the constant sign of nonlinearity induced by polymers within the model under consideration requires, in particular, a rather complex consideration of the difference in spatial structures of trans and cis isomers.

5. CONCLUSIONS

Thus, the light-induced director reorientation in an NLC with added comb-shaped polymers P1 and P2 containing light-absorbing side azo fragments and azo compound AD with a structure similar to the azo fragments was studied in detail.

It was shown that the orientational optical nonlinearity induced by the polymers is negative (the director rotates to align perpendicularly to the light field), while the sign of the AD-induced nonlinearity depends on the geometry of the interaction between the director and light field. In planar oriented samples with added polymers, all the characteristic features of the light-induced Freedericksz transition are observed.

The ratio of the induced nonlinearity to the absorbance averaged over the director orientation is larger for polymer P1, with a shorter link than that of polymer P2, and exceeds corresponding values for azo compound AD and other previously studied dyes.

It was shown that the difference in orientational optical nonlinearities caused by polymers and "free" azo molecules can be explained by a change in the symmetry of the arrangement of matrix molecules with respect to the azo fragment when the latter is bound by the polymer chain.

The results of this study show prospects for complex liquid-crystal systems containing macromolecules for increasing the efficiency of optical orientation of liquid-crystal systems.

ACKNOWLEDGMENTS

The authors are grateful to S.G. Kostromin and A.I. Stakhanov for synthesis of copolymers and azobenzene monomer AD.

This study was supported by the Russian Foundation for Basic Research (project nos. 05-02-17418 and 05-03-33193), the Federal Scientific and Technical Program (contract no. 02.434.11.2025), and the Program of Support for Young Scientists of the Presidium of the Russian Academy of Sciences (I.A. Budagovsky and M.P. Smayev).

REFERENCES

1. P. G. de Gennes, Rev. Mod. Phys. **64**, 645 (1992).
2. P. G. de Gennes, *The Physics of Liquid Crystals* (Clarendon, Oxford, 1974; Mir, Moscow, 1977).
3. L. M. Blinov, *Electro-Optical and Magneto-Optical Properties of Liquid Crystals* (Nauka, Moscow, 1978; Wiley, New York, 1983).
4. I. C. Khoo and S. L. Zhuang, Appl. Phys. Lett. **37**, 3 (1980).
5. B. Ya. Zel'dovich, N. F. Pilipetskiĭ, A. V. Sukhov, and N. V. Tabiryan, Pis'ma Zh. Éksp. Teor. Fiz. **31**, 287 (1980) [JETP Lett. **31**, 263 (1980)].
6. A. S. Zolot'ko, V. F. Kitaeva, N. Kroo, et al., Pis'ma Zh. Éksp. Teor. Fiz. **32**, 170 (1980) [JETP Lett. **32**, 158 (1980)].
7. I. Janossy, A. D. Lloyd, and B. S. Wherrett, Mol. Cryst. Liq. Cryst. **179**, 1 (1990).
8. I. Janossy, L. Csillag, and A. D. Lloyd, Phys. Rev. A **44**, 8410 (1991).
9. I. Janossy and T. Kosa, Opt. Lett. **17**, 1183 (1992).
10. M. I. Barnik, A. S. Zolot'ko, V. G. Rumyantsev, and D. B. Terskov, Kristallografiya **40**, 746 (1995) [Crystallogr. Rep. **40**, 691 (1995)].
11. A. S. Zolot'ko, V. F. Kitaeva, N. N. Sobolev, and A. P. Sukhorukov, Zh. Éksp. Teor. Fiz. **81**, 933 (1981) [Sov. Phys. JETP **54**, 496 (1981)].
12. V. F. Kitaeva, A. S. Zolot'ko, and M. I. Barnik, Mol. Mater. **12**, 271 (2000).
13. N. V. Tabiryan, B. Ya. Zeldovich, M. Kreuzer, et al., J. Opt. Soc. Am. B **13**, 1426 (1996).
14. I. A. Budagovsky, A. S. Zolot'ko, V. F. Kitaeva, and M. P. Smayev, Mol. Cryst. Liq. Cryst. **453**, 71 (2006).
15. S. M. Arakelyan, S. D. Durbin, and Y. R. Shen, Pis'ma Zh. Tekh. Fiz. **8**, 1353 (1982) [Sov. Tech. Phys. Lett. **8**, 581 (1982)].
16. I. C. Khoo and J. L. Zhuang, IEEE J. Quantum Electron. **18**, 246 (1982).
17. T. V. Galstyan and A. V. Sukhov, Zh. Tekh. Fiz. **60** (12), 81 (1990) [Sov. Phys. Tech. Phys. **35**, 1411 (1990)].
18. M. A. Venables and D. L. Tunnicliffe, J. Phys. D: Appl. Phys. **22**, 225 (1989).
19. S. H. Chen and Y. Shen, J. Opt. Soc. Am. B **14**, 1750 (1997).
20. A. Miniewicz, S. Bartkiewicz, and J. Parka, Opt. Commun. **149**, 89 (1998).
21. I. C. Khoo and Y. Liang, Phys. Rev. E **62**, 6722 (2000).
22. L. Lucchetti, M. Gentili, and F. Simoni, Mol. Cryst. Liq. Cryst. **429**, 313 (2005).
23. C. Conti, M. Peccianti, and G. Assanto, Phys. Rev. E **72**, 066614 (2005).
24. M. Peccianti, C. Conti, G. Assanto, et al., Nature **432**, 733 (2004).
25. W. Hu, T. Zhang, Q. Guo, et al., Appl. Phys. Lett. **89**, 071111 (2006).
26. A. Fratalocchi and G. Assanto, Opt. Lett. **31**, 1489 (2006).
27. A. De Luca, G. Coschignano, C. Umeton, and M. Morabito, Opt. Express **14**, 5548 (2006).
28. M. Peccianti, A. Dyadyusha, M. Kaczmarek, and G. Assanto, Nature Phys. **2**, 737 (2006).
29. J. F. Henninot, J. F. Blach, and M. Warenghem, J. Opt. A: Pure Appl. Opt. **9**, 20 (2007).
30. A. S. Zolot'ko, V. F. Kitaeva, N. Kroo, et al., Zh. Éksp. Teor. Fiz. **87**, 859 (1984) [Sov. Phys. JETP **60**, 488 (1984)].
31. A. S. Zolot'ko, V. F. Kitaeva, N. N. Sobolev, et al., Liq. Cryst. **15**, 787 (1993).
32. G. Russo, V. Carbone, and G. Cipparrone, Phys. Rev. E **62**, 5036 (2000).
33. A. Vella, A. Setaro, B. Piccirillo, and E. Santamato, Phys. Rev. E **67**, 051704 (2003).
34. I. C. Khoo and A. Diaz, Phys. Rev. E **68**, 042701 (2003).
35. B. Piccirillo, A. Vella, and E. Santamato, Phys. Rev. E **69**, 021702 (2004).
36. G. Demeter, D. O. Krimer, and L. Kramer, Phys. Rev. E **72**, 051712 (2005).
37. E. Brasselet and L. J. Dube, Phys. Rev. E **73**, 021704 (2006).
38. B. Piccirillo, A. Vella, A. Setaro, and E. Santamato, Phys. Rev. E **73**, 062701 (2006).
39. I. C. Khoo, P. Y. Yan, T. H. Liu, et al., Phys. Rev. A **29**, 2756 (1984).
40. A. J. Karn, S. M. Arakelian, Y. R. Shen, and H. L. Ong, Phys. Rev. Lett. **57**, 448 (1986).
41. J. J. Wu and S. H. Chen, J. Appl. Phys. **66**, 1065 (1989).
42. A. S. Zolot'ko and A. P. Sukhorukov, Pis'ma Zh. Éksp. Teor. Fiz. **52**, 707 (1990) [JETP Lett. **52**, 62 (1990)].
43. D. B. Terskov, A. S. Zolot'ko, M. I. Barnik, and V. G. Rumyantsev, Mol. Mater. **6**, 151 (1996).
44. E. Brasselet, B. Doyon, T. V. Galstian, and L. J. Dube, Phys. Rev. E **67**, 031706 (2003).

45. A. S. Zolot'ko, M. P. Smayev, V. F. Kitaeva, and M. I. Barnik, Kvantovaya Élektron. (Moscow) **34**, 1151 (2004).
46. A. S. Zolot'ko, A. S. Averyushkin, V. F. Kitaeva, et al., Mol. Cryst. Liq. Cryst. **451**, 41 (2006).
47. I. A. Budagovsky, A. S. Zolot'ko, N. I. Lyukhanov, et al., Zhidk. Krist. Prakt. Ispol., No. 4, 22 (2006).
48. A. M. Makushenko, B. S. Neporent, and O. V. Stolbova, Opt. Spektrosk. **31**, 741 (1971).
49. I. Janossy and E. Benkler, Europhys. Lett. **62**, 698 (2003).
50. I. Janossy and L. Szabados, Phys. Rev. E **58**, 4598 (1998).
51. V. Shibaev, A. Bobrovsky, and N. Boiko, Prog. Polym. Sci. **28**, 729 (2003).
52. T. Ikeda, J. Mater. Chem. **13**, 2037 (2003).
53. M. I. Barnik, S. A. Kharchenko, V. F. Kitaeva, and A. S. Zolot'ko, Mol. Cryst. Liq. Cryst. **375**, 363 (2002).
54. V. F. Kitaeva, A. S. Zolot'ko, and N. N. Sobolev, Usp. Fiz. Nauk **138**, 324 (1982) [Sov. Phys. Usp. **25**, 758 (1982)].
55. T. Kosa, P. Palffy-Muhoray, H. Zhang, and T. Ikeda, Mol. Cryst. Liq. Cryst. **421**, 107 (2004).
56. M. Becchi, I. Janossy, D. S. Shankar Rao, and D. Statman, Phys. Rev. E **69**, 051707 (2004).
57. A. S. Zolot'ko, Pis'ma Zh. Éksp. Teor. Fiz. **68**, 410 (1998) [JETP Lett. **68**, 437 (1998)].
58. I. P. Bazarov and É. V. Gevorkyan, *Statistical Physics of Liquid Crystals* (Mosk. Gos. Univ., Moscow, 1992) [in Russian].

Translated by A. Kazantsev